Conference paper

Hannah Robinson, Alison M. Daines, Amira Brackovic, D. Bradley G. Williams*, Ian M. Sims* and Simon F.R. Hinkley*

Cu(II) complexes using acylhydrazones or cyclen for biocidal antifouling coatings

https://doi.org/10.1515/pac-2024-0203

Abstract: Copper and copper-based compounds have broad spectrum antimicrobial activity, but concerns about leaching into the environment and toxicity on non-target organisms is leading the use of copper-based coatings being restricted. Our objective was to develop coatings that used the biocidal activity of copper, but with low negative impacts by reducing its leaching into the environment. This study reports the synthesis and characterisation of copper coordinating ligands, their formulation into coatings and testing of their antibacterial activity. A polyacylhydrazone and a series of simple acylhydrazones were synthesised and coordinated to Cu(II), but were considered unsuitable due to either their poor water-solubility or high levels of copper leaching. In an alternative approach, copper was successfully chelated to the tetraazamacrocycle, cyclen, and used to synthesise Cu(II)-cyclen functionalised silica particles, which were successfully combined with commercial paint formulations. These functionalised products showed poor antibacterial activity when incorporated into epoxy coatings, probably due to the low copper content of the formulations. However, these ligands may have other applications, such as removal of heavy metals from contaminated effluent steams.

Keywords: Acylhydrazone; copper-selective ligand; functionalised silica; marine antifouling coating; POLY-CHAR 2023; tetraaza macrocycle.

Abbreviations

ADH	adipic acid dihydrazide
DiLevDEG	dilevulinoyl diethylene glycol
DiLevDEG/ADH	water-soluble polyacylhydrazone
DAp/acr	DiLevDEG/ADH polyacylhydrazone/acrylic
GLYMO	(3-glycidyloxypropyl)trimethoxysilane
$Cn(Gm)_n$	cyclen-$(GLYMO)_n$
$CnGmSiO_2$	cyclen-GLYMO-silica
ICP-MS	inductively coupled plasma mass-spectrometry
NMR	nuclear magnetic resonance spectroscopy
SEM-EDS	scanning electron microscopy/energy dispersive X-ray spectroscopy

Article note: A collection of invited papers based on presentations at the International Polymer Characterization Forum POLY-CHAR 2023, held as an online meeting based in Auckland 22 January–26 January 2023.

***Corresponding authors: D. Bradley G. Williams**, School of Chemistry and Molecular Bioscience, University of Wollongong, Wollongong, NSW 2522, Australia, e-mail: bradleywi@uow.edu.au; and **Ian M. Sims and Simon F.R. Hinkley**, The Ferrier Research Institute, Victoria University of Wellington, 69 Gracefield Road, Lower Hutt, 5040, New Zealand, e-mail: Ian.Sims@vuw.ac.nz (I. M. Sims), Simon.Hinkley@vuw.ac.nz (S. F. R. Hinkley)
Hannah Robinson, Alison M. Daines and Amira Brackovic, The Ferrier Research Institute, Victoria University of Wellington, 69 Gracefield Road, Lower Hutt, 5040, New Zealand, e-mail: Hannah.Robinson@vuw.ac.nz (H. Robinson), Alison.Daines@vuw.ac.nz (A.M. Daines), Amira.Brackovic@vuw.ac.nz (A. Brackovic)

© 2024 the author(s), published by De Gruyter. This work is licensed under the Creative Commons Attribution-NonCommercial-NoDerivatives 4.0 International License.

Introduction

The use of copper as an antimicrobial agent has been known since ancient times. Copper and its alloys are able to kill 99.9 % of pathogenic bacteria in 2 h and were officially recognised by the Environmental Protection Agency (EPA) in 2008 as the first effective metallic antimicrobial agents [1]. Elemental copper and copper compounds have a broad spectrum of antimicrobial activity against fungi, viruses, and bacteria by several mechanisms, although membrane depolarisation is considered the main way in which copper exerts toxicity [2].

Current interest in the use of copper in antimicrobial coatings is demonstrated by the steady increase in papers published and patents granted since 2000 [2]. However, the increased development and use of copper-based antimicrobials leads to concerns about copper leaching into the environment and its toxicity on non-target organisms. For instance, current marine antifouling paints usually incorporate high levels of copper (6–76 %) as a biocidal agent [3–5]. They are designed to slowly release copper at the surface of the coating, but their use is increasingly being restricted or banned due to environmental concerns about the non-target effects of leached copper [5–8]. Whilst the risk of bacteria developing resistance to copper and other metal-based antimicrobials is thought to be low there is evidence that some bacteria are developing copper tolerance and copper-resistance genes have been [9, 10]. There is clearly a need for development of novel copper and other metal-based antimicrobial products while minimizing copper leaching into the environment. Thus, our objective was to create rechargeable coatings that are either manually recharged using solutions containing copper ions, or which draw their biocidal ingredient from the environment (*e.g.* seawater) by incorporating Cu(II)-selective ligands to bind Cu(II). This would make them antimicrobial and antifouling, while addressing environmental concerns. These coatings have potential for use multiple applications such as in the marine environment, as antifouling paints, but would also have applications in the medical field, such as antimicrobial coatings against hospital-acquired infections and biofilm formation on implanted devices (*e.g.* artificial prostheses, catheters, dental implants) [11].

Here, we report the synthesis and characterisation of Cu(II) coordinating ligands and their formulation into coatings for use as modifiers in the polymeric binders. In particular, a copper additive was generated through the functionalisation of silica particles to provide a “drop-in” coating additive that could serve as a generic modifier to confer antibacterial bioactivity, optimally demonstrating compatibility with a wide range of coating compositions. Methodology was developed to test the ability of various coatings to coordinate and retain Cu(II). The level of copper leaching from each surface of the coating was assessed using a biological assay, indirectly by determining antibacterial activity during cell-based bioassay testing, and directly through quantitative measurement using inductively coupled plasma mass-spectrometry (ICP-MS). In addition, Cu(II) containing surfaces were assayed to determine the propensity for *adherence* of live bacteria. This test was to approximate how effective the copper-containing surfaces would be in decreasing long-term biofouling in settings that avoid release of a high proportion of copper into solution (solution phase being a proxy for the environment).

Materials and methods

Materials

Anhydrous solvents were obtained commercially, and Type I water (resistivity > 18.6 MΩ) was used throughout. The model ligand, 1,4,7,10-tetraazacyclododecane (cyclen), was purchased from Chem-Impex International, Inc., IL, USA, and adipic acid dihydrazide (ADH) was supplied by Allnex GmbH (formerly Nuplex Industries). For silica functionalisation reactions, silica gel (high-purity grade, pore size 60 Å, 220–440 mesh particle size, 35–75 μm particle size; Sigma-Aldrich) was dried for 24 h at 180 °C under vacuum before use. All acids used for ICP-MS analysis were double-distilled at sub-boiling temperatures in a Teflon system in-house, starting from reagent grade acids to generate quality-controlled products. The acids were distilled at the azeotropic concentration (*i.e.* 68 % w/w for HNO_3 and 20 % w/w for HCl) and then diluted, as needed, using Type I water, which was also regularly checked as a blank.

Air-sensitive reactions were performed under an atmosphere of argon. Normal-phase thin layer chromatography (TLC) was completed on aluminium sheets coated with silica gel 60 F254 (Merck) and visualised by staining or UV light. Flash chromatography was performed on a Reveleris® X2 flash chromatography system (BUCHI) using FlashPure Cartridges (BUCHI), silica (50 µm), and a gradient of ethyl acetate in petroleum ether.

The strain of bacteria used in this work was *Escherichia coli* NZRM 3647, which was handled using aseptic technique and maintained by re-streaking from the seed stock every month for single colonies on agar plates. The plates were stored at 4 °C, and the strain was stored at −80 °C in 25 % v/v glycerol in liquid medium. *E. coli* was grown at 37 °C in nutrient broth, on nutrient agar plates, or in M63 minimal medium (see Supporting Information for details). All media were stored at 2–8 °C and handled using aseptic technique, which was implemented whenever a sterile environment was required. Sterilisation of media *via* autoclaving was conducted at 121 °C for 20 min.

Analysis

All NMR spectra, including ^{1}H, ^{13}C, COSY, HSQC and HMBC experiments were recorded on a Bruker Avance 500 spectrometer or a Jeol JNM-ECZ500S spectrometer at 27 °C in deuterated solvents. The ^{1}H NMR spectra were referenced to tetramethylsilane (TMS) or the solvent peak, and the ^{13}C NMR spectra were referenced to the solvent peak. The major solvent was referenced in mixed systems. Mass spectrometry was conducted on a Waters Q-TOF Premier™ Electrospray 175 Mass Spectrometer with a MassLynx 4.1 operating system in positive mode. Samples were prepared for analysis by mixing in aqueous methanol containing trace formic acid. IR spectra were measured on a PerkinElmer Spectrum One FT-IR spectrometer with a Universal ATR sampling accessory or on a Bruker Tensor II FT-IR spectrometer with a platinum ATR sampling accessory, and NIR spectra were measured on a PerkinElmer LAMBDA 1050 UV/Vis/NIR spectrophotometer with a 3D WB Det. Module. A SpectraMax M4 Multi-Mode Microplate Reader (Molecular Devices) and Cary 50 Bio UV–Visible Spectrophotomer (Agilent) were used to obtain UV–Vis spectra, measure absorbance, or measure OD600. The functionalised silica products were analysed by an accredited chemical laboratory (Campbell Microanalytical Laboratories, University of Otago, Dunedin, New Zealand) for CHN elemental and, in some cases, for ICP-MS analyses. CHN results were reported as duplicates within 0.30 % of one another. All other metals were analysed by ICP-MS on a Thermo Scientific Element 2 sector field ICP-MS. Images and the atomic compositions of coatings were obtained with an FEI Quanta 450 scanning electron microscope (tungsten filament) positioned at a 10 mm working distance and an Apollo X Silicon Drift Detector (EDAX) for SEM-EDS. Images were taken at 200× and 800× magnification with an electron beam spot size set at 4 and an accelerating voltage of 20 kV. EDS measurements were conducted at 200× magnification with the following parameters: spot size 6 (>1000 cps), 20 kV accelerating voltage, 30 s live time, 1.6 µs amplitude time, 35–36° take-off angle, and 129 eV resolution. BET surface area analyses were conducted on a Flowsorb II 2300 Surface Area Analyser (Micromeritics) at 21.6 °C and 1027 hPa. In bacterial adherence testing, sonication was carried out with a Bandelin Sonopuls Ultrasonic Homogeniser mini20 (2.0 sonotrode, 2.5 tip). Samples were centrifuged at 3000 relative centrifugal force (RCF) in a Rotina 380 centrifuge (Hettich).

The optical densities of bacterial cultures were measured at 600 nm with a Unicam Helios UV–Vis spectrophotometer (Biolab Scientific Ltd.) in 1 mL cuvettes (1 cm path length). The appropriate growth medium was used as a blank and to dilute the sample, as needed. Graphs were created and statistical analyses were performed using GraphPad Prism 8 (GraphPad Software, Inc.) or Microsoft® Excel® for Office 365. The bacterial enumeration data were presented as the mean value ± the standard deviation (SD), and statistical analyses were conducted when there were three or more biological replicates for each sample in the experiment. To determine if the means from two data sets were significantly different from each other, a two-sample, two-tail Student's *t*-test (unequal variance) was conducted, and the difference was considered to be significant when the p-value was <0.05. For the graphs, statistical significance was denoted as follows: *$p < 0.05$, **$p < 0.01$, and ***$p < 0.001$. One-way analyses of variance (ANOVAs) were completed to determine if the differences between the means of two or more independent data sets were statistically significant, and Tukey's *post hoc* test was used to identify which groups were statistically different.

Synthesis and testing of polyacylhydrazone and simple acylhydrazones

Synthesis

A water-soluble polyacylhydrazone (DiLevDEG/ADH) was synthesised from dilevulinoyl diethylene glycol (DiLevDEG) and adipic acid dihydrazide (ADH) as described previously [12]. Simple acyldihydrazone test compounds were synthesised following the procedure of Zha and You [13] as described previously [12].

Copper chelation

The polyacylhydrazone copper complex (Cu(II)-DiLevDEG/ADH) was prepared by adding an aliquot of DiLevDEG/ADH solution (~50 % w/v; 56 µL) to $Cu(NO_3)_2{\cdot}3H_2O$ (32 mg, 0.13 mmol) dissolved in water (1 mL). The UV–Vis spectra of DiLevDEG/ADH, the Cu(II)-DiLevDEG/ADH complex, and $Cu(NO_3)_2$ (50 mM, aq) were recorded as dilute solutions.

Paint/coating formulation

A 50 % w/v aqueous solution of DiLevDEG/ADH was formulated in a commercial acrylic paint preparation as described in Daines et al. [12]: 35 % w/w of the resin was substituted by DiLevDEG/ADH to give DAp/acr. For comparison, standard acrylic paint was prepared using a conventional recipe [12]. Following formulation and drying on a surface the paints were exposed to Cu(II) and tested for their Cu(II)-retention as well as impact on bacterial growth.

Antibacterial testing

The effects of the DAp/acr and acrylic paints (±Cu(II)) on the growth of *E. coli* NZRM 3647 were determined. To wells in a 24-well plate (JET BIOFIL®), 250 µL of DAp/acr paint, acrylic paint, or a commercial marine paint (Altex Yacht and Boat Paint, Ablative Antifouling No. 5; 40–50 % w/w Cu_2O) was added, and the plate was agitated while drying, to coat the well bottoms evenly. The paints were cured at 25 °C while shaking gently for 72 h to dry, then washed with water (3 × 500 µL) and air-dried. An aqueous solution of $Cu(NO_3)_2$ (50 mM; 500 µL/well) was added to a row of wells coated with the acrylic paint ("Acrylic + Cu(II)") and a row of wells coated with the DAp/acr paint ("DAp/acr + Cu(II)"). Water (500 µL/well) was added to a row of uncoated wells and to rows of wells coated with the DAp/acr, acrylic and marine paints. After 24 h, all wells were washed with water (3 × 500 µL), air-dried, and sterilised with UV light for 20 min. The approximate surface area of the paint in each well was measured. An culture of *E. coli* NZRM 3647 was prepared overnight by inoculating nutrient broth (3 mL) with a colony from a nutrient agar plate and incubating for 16 h at 37 °C with shaking. This culture was diluted 1:1 v/v with nutrient broth, and an aliquot of the diluted culture (500 µL; 1.3×10^8 CFU/mL) was added to each well. The plate was incubated at 37 °C, and the OD600 of the culture in each well was measured at t = 0, 2, 4, 6, 8, 10, and 24 h to generate growth curves. The experiment was repeated independently three times.

Quantification of Cu(II) leaching

The wells in a 24-well plate were coated with DAp/acr paint, acrylic paint, or a commercial marine paint as described above. Nutrient broth (500 µL) was added to each well and the plate was incubated at 37 °C for 24 h. The supernatant was removed from each well, diluted 10,000× with nitric acid (3 % v/v aq), and analysed by ICP-MS to quantify the copper that had leached into the nutrient broth.

Assessment of DiLevDEG/ADH polyacylhydrazone leaching

The bottom of a well in a 24-well plate was coated evenly with 260 mg of the DAp/acr paint and was cured at 50 °C for 24 h. The cured paint was washed with water (3×), air-dried and deuterium oxide (500 µL) was added and left for 24 h. The ^{13}C NMR spectrum of the resulting deuterium oxide solution was recorded and compared to the spectrum of DiLevDEG/ADH polyacylhydrazone.

Synthesis and testing of silica-cyclen-copper complexes

Functionalisation of silica with cyclen

Two methods were utilised for the functionalisation of silica with cyclen (1,4,7,10-tetraazacyclododecane), as shown in Scheme 1. The difference in these two methods is the order in which the particle-ligand system is built, but is ultimately intended to produce identical products. Detailed methodology is provided in the Supplementary Information.

For **Method 1**, four procedures were trialled for synthesis of GLYMO-silica ($CnGmSiO_2$) as summarised in Table 1. Subsequent functionalisation with cyclen was modelled on the procedure of Gros et al. [14]. Briefly, $GmSiO_2$ was end-capped by suspending in trimethylchlorosilane (TMCS; 92 mmol) and heating at reflux temperature for 4.25 h under argon. The silica product was vacuum filtered, washed with water to neutral pH, and dried for 18 h under high vacuum. Next, an aqueous solution of cyclen (59 mL, 3.3 mmol) in water was added to the end-capped $GmSiO_2$ and the suspension heated at 80 °C for 48 h with occasional gentle swirling. The resulting product was filtered to remove excess cyclen and was washed with dilute hydrochloric acid (0.1 M; 2 × 10 mL), then water (until the filtrate no longer turned a dark blue colour upon the addition of 50 mM $CuSO_4$), and hot methanol.

For **Method 2**, six procedures were trialled for the synthesis of cyclen-GLYMO ($Cn(Gm)_n$) as summarised in Table 2. Immobilisation of $Cn(Gm)_n$ on to silica was done in the presence or absence of $Cu(NO_3)_2$ to produce preloaded Cu(II)-$CnGmSiO_2$ and free, uncoordinated $CnGmSiO_2$ (Table 2). A solution of $Cu(NO_3)_2$ in methanol was

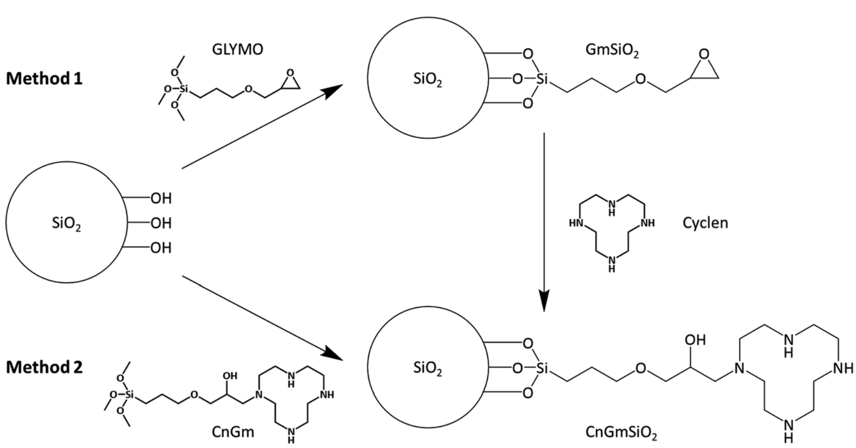

Scheme 1: Two silica functionalisation methods. Method 1: reaction between GLYMO and the silanol groups of silica (SiO_2) to produce GLYMO-functionalised silica ($GmSiO_2$). Then, the reaction between $GmSiO_2$ and cyclen to produce cyclen-GLYMO-silica ($CnGmSiO_2$). Method 2: GLYMO and cyclen react first to produce cyclen-GLYMO (CnGm), and then CnGm reacts with silica to produce $CnGmSiO_2$.

Table 1: Reaction conditions for $GmSiO_2$ synthesis.

Conditions	Procedure 1	Procedure 2	Procedure 3	Procedure 4
SiO_2 (g)	0.91 (dry)	1.02 (dry)	1.00 (wet)	2.50 (dry)
GLYMO (g, mmol)	0.27, 1.1	2.1, 9.1	4.3, 18	3.7, 16
Anhydrous toluene (mL)	5	4	–	35
Triethylamine (µL)	–	–	–	75
Temperature (°C)	20 (RT)	80	100	110.6 (reflux)
Time (h)	24	72	69	42

Table 2: Reaction conditions for $Cn(Gm)_n$ synthesis.

Conditions	Procedure 1	Procedure 2	Procedure 3	Procedure 4	Procedure 5	Procedure 6
GLYMO (mmol)	4.4	1.1	2.3	1.1	1.1	8.9
Cyclen (mmol, eq)	1.1, 0.26	4.8, 4.3	0.56, 0.25	1.2, 1.1	1.2, 1.1	9.7, 1.1
$Al(OTf)_3$ (mmol)	–	–	–	0.1	0.1	–
Solvent	2:1 $MeOH:H_2O$	Toluene	Toluene	$CHCl_3$	$CHCl_3$	$CHCl_3$
Volume solvent (mL)	23.8	7.5	10	2	2	16
Temperature (°C)	20 (RT)	110.6 (reflux)	110.6 (reflux)	20 (RT)	20 (RT)	20 (RT)
Time (h)	5	24	97.5	90	69	8–10 days
Reference	[16]	[17]		[18]		–

added to the crude $Cn(Gm)_n$ for copper incorporation into the ligand. Then, methoxysilane groups were hydrolysed following the procedure of Lu [15]. Briefly, methanol, aqueous ammonium hydroxide (28 % v/v) and silica (26.68 g) were added to the reaction mixture, and stirred and heated for 1 h at 60 °C. The mixture was concentrated under vacuum and the royal blue Cu(II)-$CnGmSiO_2$ product was washed by Soxhlet extraction with water for 24 h, then dried. Uncoordinated $CnGmSiO_2$ was prepared in the same way, but without addition of copper(II) nitrate.

Incorporation of $CnGmSiO_2$ into coatings

A two-pack epoxy was prepared by mixing a commercial hardener (Ancamine® 2459 Curing Agent; Air Products and Chemicals, Inc., PA, USA) and a commercial epoxy resin (Epikote™ 235; Resolution Performance Products, Columbus, OH, USA) in accordance with the manufacturer specifications: 0.563 g Ancamine® 2459/g Epikote™ 235. Immediately following manual mixing of the two components, one coat of the viscous, dark yellow epoxy resin was applied to a single side of a black vinyl chloride/acetate copolymer (black scrub test panel, Leneta). An inverted funnel was then used to add silica to a defined surface area of the still-uncured resin so that, at minimum, one layer of silica covered the resin. The coating was allowed to cure at room temperature overnight, and, the following day, the procedure was repeated for the second side. After allowing the second side to cure at room temperature overnight, the silica/epoxy (SiO_2/epx)-type samples were brushed, washed with water, and dried with compressed air, and squares (23 mm × 23 mm) coated on both sides were cut from the material. These squares were tested immediately for bacterial adherence. The four silica samples prepared for testing were as follows: 1) $CnGmSiO_2$ (free ligand), 2) $CnGmSiO_2$ + Cu(II) (post-loaded), 3) Cu(II)-$CnGmSiO_2$ (pre-loaded), and 4) unfunctionalised SiO_2. To post-load $CnGmSiO_2$, the squares coated on both sides with $CnGmSiO_2$ were submerged in an aqueous solution of an excess of $Cu(NO_3)_2$ (50 mM; 16.5 mL) for 24 h, washed with water, dried with compressed air, and tested immediately for bacterial adherence. Images and the elemental composition of the SiO_2/epx-type coatings were obtained by SEM-EDS.

Bacterial adherence assay

The ability of the coatings to deter the adherence of bacteria was assessed by determining the attachment of *E. coli* NZRM 3647. An uncoated sample square and sample squares coated with the commercial epoxy resin and marine paint were also tested. An overnight culture was prepared by inoculating nutrient broth (3 mL) with a colony of *E. coli* NZRM 3647 from a nutrient agar plate and incubating for 16 h at 37 °C with shaking. The squares were sterilised with UV light for 20 min per side in a laminar flow hood, and then each of the sterilised squares were submerged in overnight culture diluted with M63 minimal medium to OD600 0.05 (final volume 16.5 mL; 5 ± 2 ($\times 10^7$) CFU/mL). The diluted cultures were incubated 24 h at 37 °C without shaking. Following incubation, the OD600 of each culture was measured, and the squares were transferred to sterile saline (20 mL) for 5 min to remove planktonic bacteria. A pipet was used to rinse both sides of the squares with sterile saline (500 µL/side) before transferring the squares to tubes containing sterile solutions of 0.05 % v/v Tween 20 in saline (final volume 20.0401 mL). These solutions were vortexed 2 min at maximum speed and sonicated 8 s at 40 % amplitude to detach bacteria from the squares. Serial dilutions (10×) of the solutions were performed to count colonies by the drop plate method. The experiment was independently repeated three times.

Measurement of copper leaching

The concentrations of copper leachate from $CnGmSiO_2$ + Cu(II)/epx, Cu(II)-$CnGmSiO_2$/epx, and the marine paint were determined by incubating the test squares in M63 minimal medium statically for 24 h at 37 °C. This experiment was conducted with and without *E. coli* in order to determine if the presence of bacteria affected copper-leaching. After 24 h incubation of the samples with *E. coli*, each culture was filter-sterilised and centrifuged, and the supernatant was isolated for analysis. All solutions were diluted, as needed, with dilute nitric acid for copper quantification by ICP-MS.

Results and discussion

Polyacylhydrazone and simple acylhydrazones

We previously synthesised a water-soluble polyacylhydrazone from dilevulinoyl diethylene glycol (DiLevDEG) and adipic acid dihydrazide (ADH) and incorporated it as part of the resin into a commercially available acrylic paint [12]. For the present study, we postulated that the acylhydrazone functionality of DiLevDEG/ADH had the potential to coordinate Cu(II) in a five-membered chelate ring by bidentate coordination through the carbonyl oxygen and azomethinic nitrogen atom (Fig. 1).

Following synthesis of DiLevDEG/ADH, addition of $Cu(NO_3)_2$ to an aqueous solution gave a colour change that indicated Cu(II)-coordination due to modification of the d-d transitions, in which the excitation of an electron from a lower-energy to a higher-energy d-orbital (*i.e.* $t_{2g} \rightarrow e_g$) occurs [19]. The UV–Vis spectrum provided further evidence of Cu(II)-chelation by the DiLevDEG/ADH polyacylhydrazone with absorption at both higher (λ_{max} = 782 nm) and lower (shoulder starting below ~470 nm) wavelengths compared with DiLevDEG/ADH alone which absorbed at lower wavelengths, beginning around 420 nm (Figs. 2 and 3).

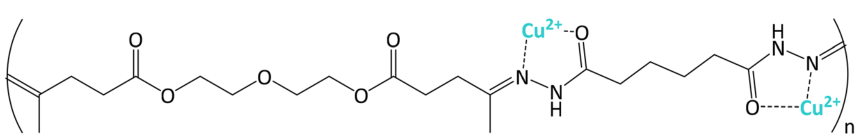

Fig. 1: Proposed Cu(II)-chelation by the acylhydrazone functionality in DiLevDEG/ADH.

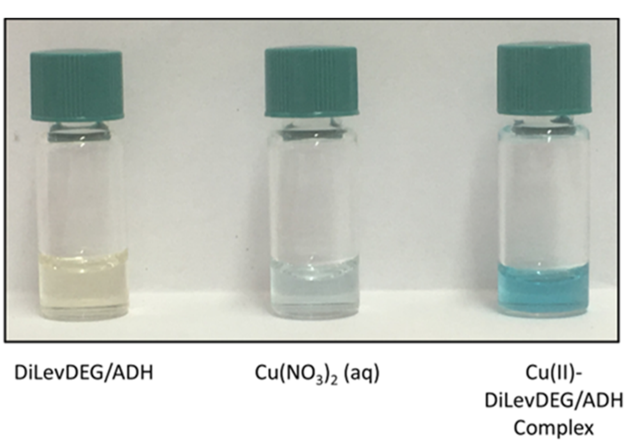

Fig. 2: Colour change of the aq DiLevDEG/ADH solution upon the addition of $Cu(NO_3)_2$, caused by d–d transitions ($t_{2g} \rightarrow e_g$; Δ_0 = crystal field splitting).

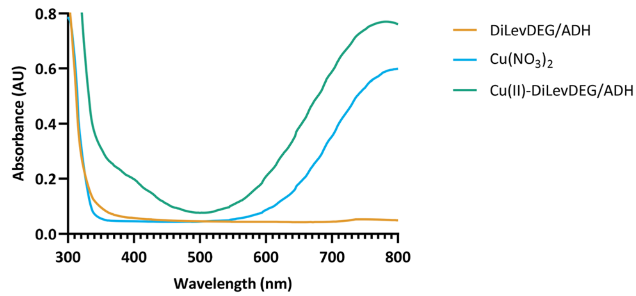

Fig. 3: UV–Vis spectra of DiLevDEG/ADH, $Cu(NO_3)_2$, and Cu(II)-DiLevDEG/ADH.

Next, DiLevDEG/ADH was formulated into a paint (DAp/acr) with 35 % w/w substitution of the resin and, following exposure to $Cu(NO_3)_2$, tested for its ability to bind and retain Cu(II) and its ability to inhibit bacterial growth. The growth of *E. coli* NZRM 3647 was assessed when in contact with the acrylic paint (with or without Cu(II)), 35 % w/w DAp/acr paint (with or without Cu(II)), and a commercial marine paint (Fig. 4).

Unexpectedly, the Acrylic + Cu(II) coating displayed greater growth inhibition than both the marine and DAp/acr + Cu(II) paints. Since release of copper ions is necessary for antimicrobial activity in this assay, a weaker association of Cu(II) in the Acrylic + Cu(II) paint compared with the DAp/acr + Cu(II) paint could explain the differences in antibacterial activity between these coatings. To test this hypothesis, ICP-MS measurement of the amount of copper leached from paint into the nutrient broth after 24 h (Table 3) was performed, and showed that the Acrylic + Cu(II) paint had leached the greatest amount of copper and the marine paint the least, suggesting that the inhibition of *E. coli* NZRM 3647 growth was related to the amount of Cu(II) released. The DAp/acr + Cu(II) paint had an approximately equivalent inhibitory effect to the marine paint, however, this effect was also attributed to its release of copper which was higher than for the marine paint.

In addition to growth inhibition by the copper-containing paints, we also observed considerable inhibition by DAp/acr without Cu(II). This suggested that there was leaching of the DiLevDEG/ADH polyacylhydrazone from the coating, and that this species may also have antimicrobial activity. Leaching of the DiLevDEG/ADH polyacylhydrazone binder was confirmed by comparing the ^{13}C NMR spectrum of the leachate with that of DiLevDEG/ADH (Fig. 5).

Resonances for **C2** (C=N) were observed at 163.0 and 159.1 ppm, and the signal for **C5**, the hydrazone carbonyl, was observed at 173.1 ppm. The signal ratio of end-group **C6** to **C4** was approximately 1:4 in the leachate spectrum compared with 1:11 in the reference spectrum, indicating that the polyacylhydrazone was releasing small

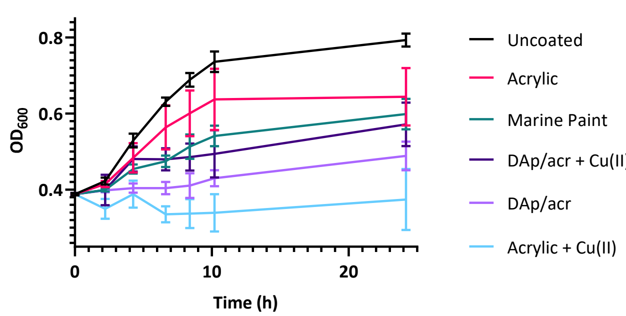

Fig. 4: Growth curves (OD_{600} vs. time) of *E. coli* NZRM 3647 in uncoated wells and wells coated with the acrylic (±Cu(II)), 35 % w/w DAp/acr (±Cu(II)), and marine paints. The error bars show the standard deviation (SD) from three biological replicates.

Table 3: Amounts of copper leached into nutrient broth after 24 h from Cu(II)-loaded paints and commercial marine paint.

Coating	Cu (ppm)	Cu (μg)	Cu (mM)
Acrylic + Cu(II)	180 ± 10[a]	91 ± 5	2.9 ± 0.2
DAp/acr + Cu(II)	80 ± 10	39 ± 5	1.2 ± 0.2
Marine paint	50 ± 1	25.2 ± 0.6	0.79 ± 0.02

[a]Mean ± SD, n = 3. ppm = μg/mL, μg/g.

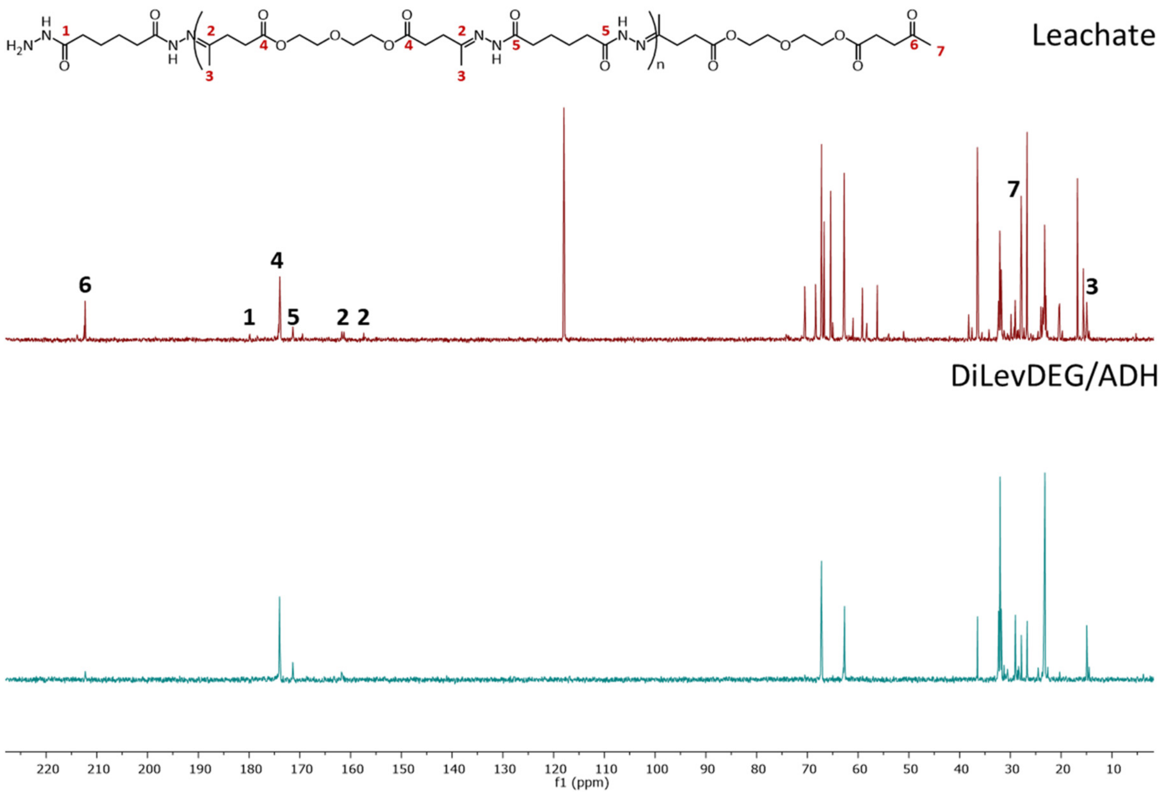

Fig. 5: ^{13}C NMR spectra (crude; D_2O) of the leachate (top) and DiLevDEG/ADH polyacylhydrazone (bottom) with select carbon assignments (δ_C 118.0 ppm = acetonitrile).

molecules and/or monomers into solution. Other resonances not attributed to DiLevDEG/ADH were observed in the spectrum of the leachate, indicating that other unidentified compounds were also leached from the DAp/acr paint.

Overall, these results revealed that the DAp/acr paint was unsuitable as an antifouling coating. Nevertheless, the ability of the polyacylhydrazone to coordinate Cu(II) and its successful formulation into a paint, suggested that simple acylhydrazones may be suitable as a candidate Cu(II)-ligand class for antifouling coatings. Encouragingly, there is separate evidence that Cu(II)-acylhydrazone complexes have antimicrobial activities, with 2-thiophenecarbonyl hydrazone of 3-isatin bound to Cu(II) showing antibacterial activity against both Gram-positive and Gram-negative bacteria [20]. Consequently, a series of acylhydrazones were synthesised (Scheme S1, Supporting Information) using standard chemistry [13], the anticipated structures of which were confirmed by NMR spectrometry and supported by high-resolution mass spectrometry (HRMS) (Supporting Information). Disappointingly, the products were only soluble in dipolar aprotic solvents (DMF and DMSO), and their poor water-solubility rendered them unsuitable for formulation in paint coatings.

Cyclen and cyclen-modified silica

Given the unsuitability of acylhydrazones for our purposes, we therefore turned our attention to tetraaza/oxatriaza macrocycles (specifically cyclen, 1,4,7,10-tetraazacyclododecane) as an alternative Cu(II) ligand class due to their Cu(II)-selectivity, antimicrobial activity, favourable $K_{\mathrm{Cu(II)L}}$ values, and more suitable solubility profiles. These types of compounds have shown excellent performance as ligands for various metals and can be functionalised with side arms that permit their other characteristics to be modified without impeding their ability to chelate metals [11, 21–26].

To start, cyclen and $CuCl_2$ were allowed to react in MeOH for 2 h yielding a dark blue precipitate. ESI-HRMS afforded *m/z* 234.0916 consistent with a 1:1 Cu(II):cyclen complex ($C_8H_{19}CuN_4$ $[M–H]^+$). The UV–Vis spectrum of the Cu(II)-cyclen complex showed an absorption peak with λ_{max} = 590 nm, similar to that reported for other Cu(II)-cyclen derivative complexes [27, 28]. To incorporate cyclen into a coating binder, several combinations of amine and/or alcohol components with a cycloaliphatic diisocyanate (Desmodur® W (Covestro)) were trialled to produce polyurea or polyurethane coatings, respectively (Scheme S2, Table S1). However, these combinations resulted in polymers that displayed physical characteristics that were unsuited to coatings or showed no observable polymerisation at all (Table S2). Similarly, trials to incorporate cyclen, cyclam, DETA, and PEI, respectively, as curing agents and/or surface-modifiers in a two-pack epoxy system resin (Epikote™ 235) produced coatings with undesirable physico-mechanical properties, making them unsuitable as an antifouling coating (Tables S3, S4 and S5; Scheme S3). Therefore, we sought alternative methods of incorporating the Cu(II)-ligand complexes, specifically considering silica, which is already widely employed in the coatings industry.

Cyclen modified silica

Silica is a low-cost, common additive and extender that can enhance multiple properties of coatings and is found in several coating types, including antifouling coatings. Mesoporous silica nanoparticles functionalised with quaternary ammonium salts and formulated into a coating, have been found to reduce biofouling coverage from 39 % to below 10 % [29]. These results suggested that modified silica particles are rich with potential to serve as functional fillers in antifouling coatings. The known positive influence of silica on the physical characteristics of the coatings, together with their existing demonstrated antifouling characteristics, led us to consider this material as a solid support for the cyclen ligands and/or Cu-complexes. The incorporation of cyclen in a coating through the modification of silica, was considered as a flexible strategy since copper loading could, in theory, be undertaken before or after formulation into a surface coating. In addition, the inclusion of aza-macrocycles into surface coatings using silica particles should reduce leaching of the loaded copper into seawater (due to the macrocycle's high copper affinity), while still presenting copper ions at the surface of the coating at its coating-liquid interface [30].

Two methods were trialled for functionalisation of silica with the cyclen ligand; method 1 in which the reaction between GLYMO and the silanol groups of silica gives $GmSiO_2$, and then the reaction between $GmSiO_2$ and cyclen produces $CnGmSiO_2$; method 2 where GLYMO and cyclen react first to produce CnGm, and then CnGm reacts with silica to produce $CnGmSiO_2$. All attempts to synthesise $CnGmSiO_2$ via method 1 were unsuccessful. Several procedures for the synthesis of $GmSiO_2$ were evaluated and the outcomes are summarised in Table 4. Procedure 1 yielded mostly unreacted GLYMO with almost no functionalisation of the silica. The other procedures yielded $GmSiO_2$ with varying degrees of functionalisation, but only procedure 4 showed evidence of silica modification (appearance of the epoxy ring C–O stretch peak at 908–920 cm^{-1} in the IR spectrum; Fig. S1, Table S6). Unfortunately, attempts to end-cap $GmSiO_2$ and subsequent synthesis of $CnGmSiO_2$ were unsuccessful, as determined by IR spectroscopy.

Turning to the synthesis of $CnGmSiO_2$ via method 2, several procedures were trialled to synthesise $Cn(Gm)_n$ (Scheme 2, Table 2). Most of the procedures trialled were unsuccessful and only the reaction of GLYMO with cyclen (1.1 eq) in anhydrous chloroform at room temperature under dry conditions and an argon atmosphere (Table 2,

Table 4: Method 1 outcomes of $GmSiO_2$ synthesis using different procedures as shown in Table 1.

Outcomes	Procedure 1	Procedure 2	Procedure 3	Procedure 4
GLYMO filtrate (g)	0.27	2.0	3.8	2.7
GLYMO – GLYMO filtrate (g)	0.003	0.2	0.5	1.0
GLYMO recovered (%)	99	92	89	73
$GmSiO_2$ (g)	0.97	1.18	1.40	3.17
$GmSiO_2 – SiO_2$ (g)	0.06	0.16	0.40	0.67
$GmSiO_2$: mmol GLYMO/g SiO_2	0.01	0.65	1.7	1.1
Functionalisation (%)[a]	1	65	170	110

[a]The percent functionalisation was calculated by comparing mmol GLYMO/g SiO_2 to the ideal (0.991 mmol modifier/g SiO_2) [31].

procedure 6), showed the reaction go to completion. This was evident in the ^{1}H NMR spectra of the recovered product (Fig. 6) from the disappearance of the resonance associate with the H2 proton of the epoxide at δ_H 3.14. The presence of the CnGm product was confirmed by HRMS (*m/z* calcd for $C_{17}H_{41}N_4O_5Si$ [CnGm + H]$^+$ 409.2846; found 409.2843). The regioselectivity of the ring-opening reaction was determined through 2-D NMR experiments (HSQC; (^{1}H, ^{13}C)- and (^{1}H, ^{15}N)-HMBC; COSY) (Figs. S2 and S3).

The CnGm product was then taken for synthesis of CnGmSiO$_2$ and pre-loaded Cu(II)-CnGmSiO$_2$ (Scheme 3). To create the preloaded Cu(II)-CnGmSiO$_2$, first excess of copper(II) nitrate (aq, light blue solution) was added to the CnGm reaction mixture in chloroform and the complexation was evidenced by the colour change of the reaction mixture from colourless to dark blue. Initial attempts to synthesise Cu(II)-CnGmSiO$_2$ using 0.05 % v/v aqueous ammonium hydroxide at room temperature to hydrolyse the GLYMO methoxy groups followed by addition of

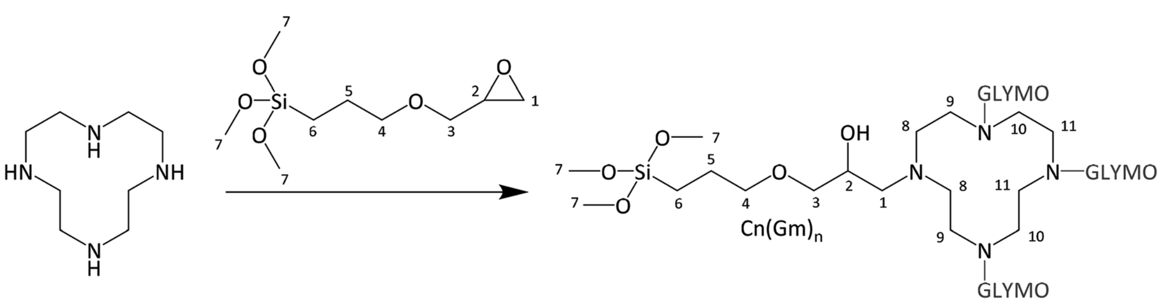

Scheme 2: Synthesis of Cn(Gm)$_n$.

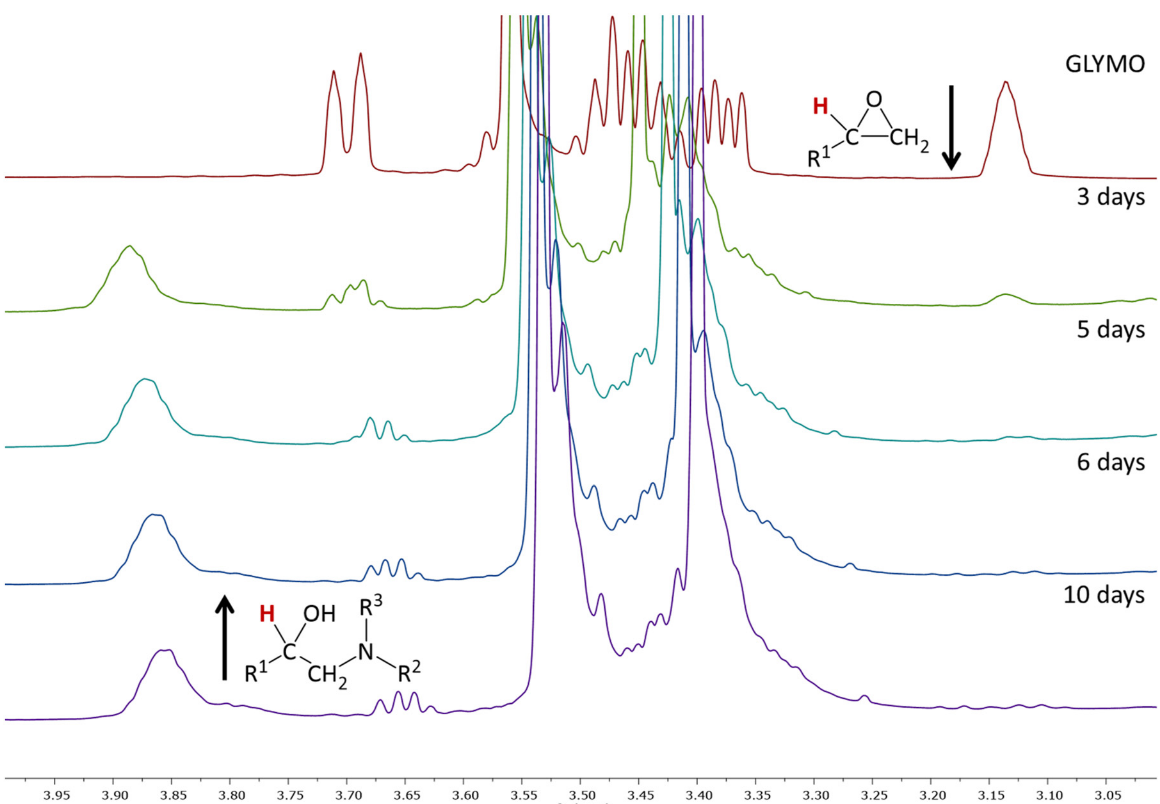

Fig. 6: ^{1}H NMR spectra (CDCl$_3$, δ_H 4.00–3.00 ppm) of GLYMO and the samples at 3, 5, 6, and 10 days from the Cn(Gm)$_n$ procedure 6 reaction mixture, showing the change in the spectrum with the progression of the ring-opening reaction. H is the proton responsible for the indicated peak.

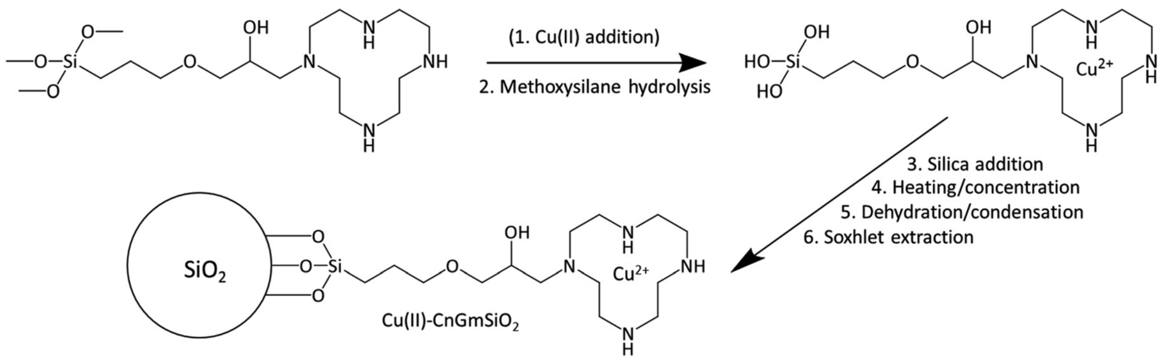

Scheme 3: In order to synthesise Cu(II)-CnGmSiO_2, Cu(II) may be added first to produce the Cu(II)-CnGm complex **(1)**. Then, hydrolysis of the methoxysilane groups **(2)** is followed by the addition of silica **(3)** and heating and concentration **(4)** to drive the dehydration/condensation reaction **(5)**. Finally, the ±Cu(II)-CnGmSiO_2 product is washed via Soxhlet extraction **(6)**.

silica, concentration of the reaction mixture under vacuum while heating, and Soxhlet extraction yielded a royal blue Cu(II)-CnGmSiO_2 product. CHN analysis of the product revealed a percent functionalisation of the silica was only 32 %. We hypothesised that this low degree of functionalisation was due, at least partly, to incomplete hydrolysis of the GLYMO methoxy groups which would preclude subsequent silica modification. Monitoring the hydrolysis in 0.05 % v/v aqueous ammonium hydroxide at room temperature showed that while 78 % of the methoxy groups were hydrolysed within 0.2 h, hydrolysis was still incomplete after 4.7 h (Fig. 7).

Increasing the percentage of ammonium hydroxide to 1 % v/v (CD_3OD, 3.7 % v/v H_2O, 11 % v/v $CHCl_3$) and heating at 60 °C gave almost complete hydrolysis of the methoxy groups in 1 h. Subsequent addition of silica and concentration of the mixture under vacuum promoted the dehydration/condensation reactions, and Soxhlet extraction of the product yielded dark blue Cu(II)-CnGmSiO_2. The degree of functionalisation of this silica was

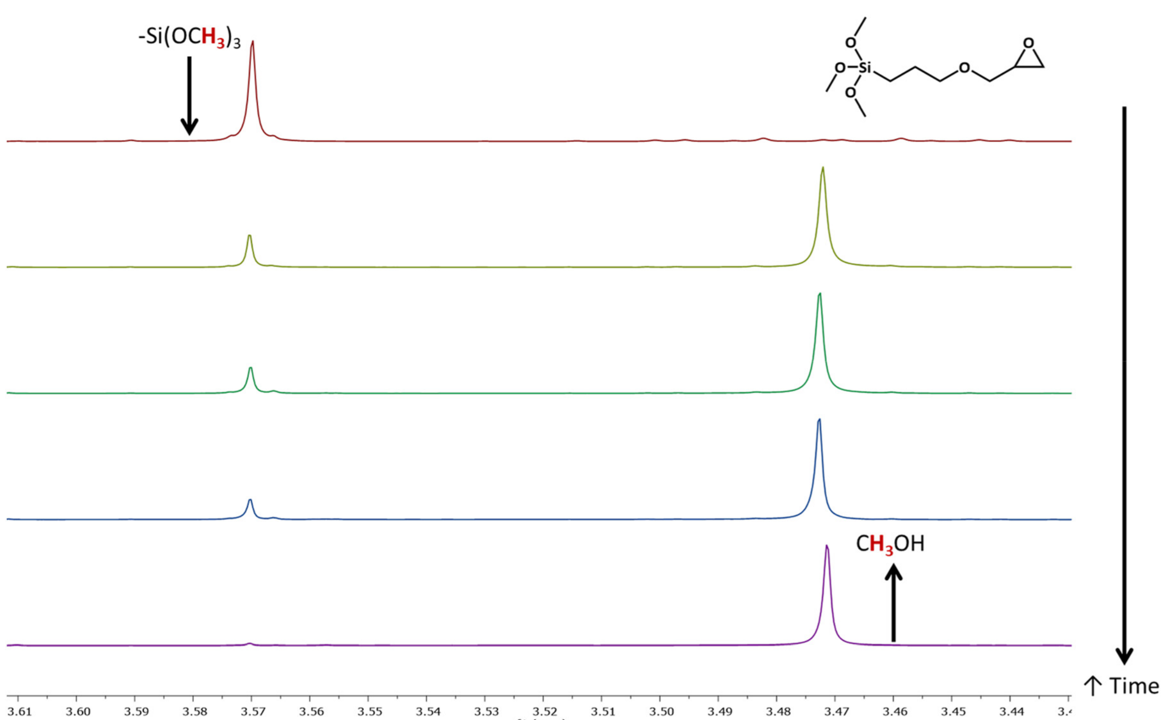

Fig. 7: ^1H NMR spectra ($CDCl_3$) of GLYMO (δ_H 3.61–3.43 ppm), following methoxy group hydrolysis over time.

73 %. A similar degree of functionalisation was observed for the two batches of $CnGmSiO_2$, 75 and 88 % functionalisation respectively.

Measurement of the copper content of the two pre-loaded batches of Cu(II)-$CnGmSiO_2$ products showed that the one with higher degree of functionalisation had 2.60 % copper, compared with 0.48 % for the one with a lower degree of functionalisation. After exposure of the $CnGmSiO_2$ products to aqueous $Cu(NO_3)_2$ solutions for 24 h (post-loading with Cu(II)) the measured copper contents were 0.96 % w/w and 1.02 % w/w, respectively. Previous studies found that harsh conditions (2–3 h refluxing in ethanol with an excess of Cu(II)) were necessary for complete metallation of cyclam-modified silica [32–34], which may account for the lower loading obtained for post-loading with Cu(II) compared with pre-loaded Cu(II)-$CnGmSiO_2$.

These functionalised silica products were incorporated into coatings using a two-pack epoxy system, composed of an epoxy resin and a commercial hardener. Resins containing $CnGmSiO_2$ were post-loaded with Cu(II) by submerging in an aqueous solution containing an excess of $Cu(NO_3)_2$ for 24 h, washed with water and dried. Magnified images of the SiO_2/epx-type coatings scanning electron microscopy revealed consistent, but inhomogeneous, surface coverage with the functionalised silica products and photographs of the prepared squares are shown in the top left-hand corner (Fig. 8). Analysis of the elemental compositions of the coatings obtained via scanning electron microscopy/energy dispersive X-ray spectroscopy (SEM-EDS) showed the presence of the copper, although the results varied compared to the ICP-MS analysis of silica products due to the inhomogeneity of the surfaces: (1.02 % w/w (ICP-MS) vs. 1.0 % (SEM-EDS) for $CnGmSiO_2$ + Cu(II)/epx and 2.60 % w/w (ICP-MS) vs. 1.4 % w/w (SEM-EDS) for Cu(II)-$CnGmSiO_2$/epx copper (Tables S7 and S8).

The ability of these coatings to deter the adherence of bacteria was assessed by determining the attachment of *E. coli* (NZRM 3647). The results of the assay showed that there was no deterrence of bacterial adhesion on any of the functionalised silica coatings (Fig. 9), including the biocide-containing $CnGmSiO_2$ + Cu(II)/epx and Cu(II)-$CnGmSiO_2$/epx coatings. Interestingly, Cu(II)-$CnGmSiO_2$/epx had the greatest number of viable, adherent bacteria, and this result was statistically different from the adherence results for all of the other coatings but SiO_2/epx. The

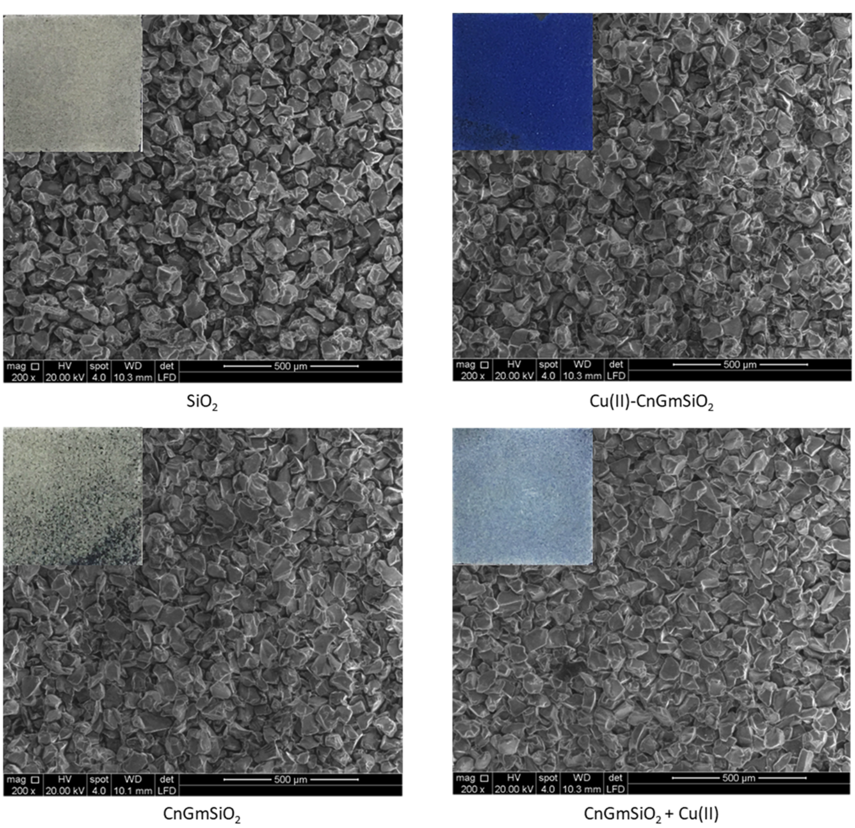

Fig. 8: SEM secondary electron images at 200× magnification of the SiO_2/epx-type squares to be tested for bacterial adherence (HV 20 kV, spot size 4, WD 10 mm, LFD). The coatings include SiO_2/epx, Cu(II)-$CnGmSiO_2$/epx (preloaded), $CnGmSiO_2$/epx, and $CnGmSiO_2$ + Cu(II)/epx (postloaded), and pictures of these coatings are in the top left corner of each SEM image.

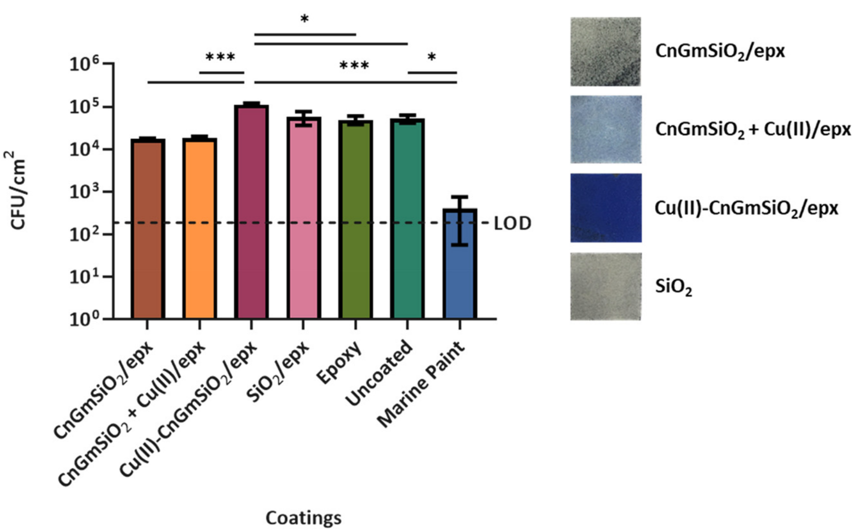

Fig. 9: Results of *E. coli* NZRM 3647 CFU/cm^2 on the SiO_2/epx-type coatings (pictured right), as well as on uncoated squares, the epoxy resin, and the marine paint. The bars represent the mean (biological replicates = 6 for “Uncoated”, biological replicates = 3 for all others) ± SD. To determine if the means from the data sets were significantly different from each other, a one-way ANOVA with Tukey’s *post hoc* test was conducted, and the difference was considered to be significant when the *p*-value was <0.05 (*$p < 0.05$, **$p < 0.01$, ***$p < 0.001$; LOD = 106 CFU/cm^2).

number of bacteria attached to Cu(II)-CnGmSiO_2/epx was approximately six-fold higher than the number for CnGmSiO_2/epx and CnGmSiO_2 + Cu(II)/epx and approximately twice the number for SiO_2/epx. This was unexpected, given that Cu(II)-CnGmSiO_2 had the highest % w/w copper (2.6 %) out of all of the SiO_2/epx-type coatings. The marine paint gave the lowest CFU/cm^2 (±SD), at the LOD of the assay, and none of the other coatings had comparable activity.

In order to investigate possible factors impacting the adherence results, the amount of copper leaching from each copper-containing coating into the medium during the 24 h incubation was measured, both in the presence and absence of *E. coli* (Table 5). Although the copper concentrations in the marine paint (40–50 % w/w) and Cu(II)-CnGmSiO_2 (2.6 ± 0.3 % w/w) were vastly different, the concentrations of copper leachate in the absence of *E. coli* were statistically equivalent: 3.3 ± 0.5 ppm (52 ± 8 μM) and 3.6 ± 0.3 ppm (57 ± 5 μM). The concentration of copper leached from CnGmSiO_2 + Cu(II)/epx was slightly lower (2.3 ± 0.1 ppm, 36 ± 2 μM) than the other coatings when bacteria were absent. Interestingly, the presence of bacteria resulted in increased copper-leaching for all samples, and CnGmSiO_2 + Cu(II)/epx leached the most copper (12 ± 2 ppm, 190 ± 30 μM), while the marine paint (7.3 ± 0.4 ppm, 115 ± 6 μM) and Cu(II)-CnGmSiO_2/epx (6.0 ± 0.4 ppm, 94 ± 6 μM) leached similar, lower amounts. This increase in copper-leaching in the presence of *E. coli* could be due to the uptake of Cu(II) from the surface by bacteria, since cations are attracted to the negatively charged lipopolysaccharide (LPS) in the outer membrane [35, 36].

Table 5: The OD_{600} of the *E. coli* cultures after 24 h incubation and the copper content of the test squares, as well as the copper-leachate concentrations after 24 h.

Coating	OD_{600} (24 h, M63)[a]	% w/w Cu[b]	ppm (μM) Leached Cu[a]
CnGmSiO_2/epx	0.119 ± 0.007	0	–
CnGmSiO_2 + Cu(II)/epx	0.057 ± 0.003	1.0 ± 0.3[a]	2.3 ± 0.1 (36 ± 2)[c], 12 ± 2 (190 ± 30)[d]
Cu(II)-CnGmSiO_2/epx	0.072 ± 0.003	2.6 ± 0.3[a]	3.6 ± 0.3 (57 ± 5)[c], 6.0 ± 0.4 (94 ± 6)[d]
SiO_2/epx	0.116 ± 0.004	0	–
Epoxy	0.151 ± 0.008	–	–
Uncoated	0.148 ± 0.009	–	–
Marine paint	0.101 ± 0.006	40–50	3.3 ± 0.5 (52 ± 8)[c], 7.3 ± 0.4 (115 ± 6)[d]

[a]Mean ± SD. Experiment repeated 3×. [b]% w/w Cu in the (un)functionalised silica component or in the marine paint. [c]M63 minimal medium without *E. coli* NZRM 3647. [d]M63 minimal medium with *E. coli* NZRM 3647.

Copper leachate concentrations were measured because they were thought to be relevant to the bacterial adherence results, but there was not a straightforward relationship between the two. The marine paint and Cu(II)-CnGmSiO_2/epx leached the same amount of copper (94–115 µM, Table 5), but there was an almost 3 Log_{10} reduction in the number of viable, adherent bacteria when the test square was coated with the marine paint instead of Cu(II)-CnGmSiO_2/epx (Fig. 9).

The mechanisms of the contact killing of bacteria on a copper surface are not fully understood, but there is a consensus in the literature that copper ions released from the surface play a role [9, 37, 38]. It is proposed that, following damage to the bacterial cell membrane, the influx of copper ions into the cell causes oxidative damage by ROS and enzyme inhibition, leading to cell death and DNA degradation [37,39]. In culture, copper toxicity is due to the displacement of iron by copper in iron-sulfur cluster dehydratases, which are essential for the branched-chain biosynthesis of amino acids [40].

The unexpected results of the bacterial adhesion assays may be attributed to the relationship that exists between surface roughness and bacterial colonisation. Rough surfaces have a greater surface area for bacterial adhesion and can provide shelter from shear forces that would otherwise remove the bacteria [41]. However, it was observed that at the appropriate biocide concentration, even if the surface is rough, bacterial adhesion will be deterred. Kozlovsky et al. [42] assessed antibacterial activity (against *Streptococcus mutans*) of chlorohexidine (CHX) on titanium disks that were either sand-blasted, acid-etched or machine-smoothed. Greater surface area of the rough disk provided more sites for adsorption of CHX resulting in improved antibacterial activity compared to smooth surface [42]. Therefore, in future work we aim to achieve a high enough copper concentration at the silica surface to overcome the positive effect of the rough surface on bacterial growth.

Conclusions

In conclusion, we present the synthesis of Cu(II)-selective ligands for the development of antimicrobial coatings. With the cyclen-based ligands we have shown they can be attached to silica and mixed with commercial paint formulations. Testing the adherence of *E. coli* to the SiO_2/epx-type coatings revealed that the functionalised silica coatings, with and without Cu(II), did not deter cellular attachment. This could be due to relatively low copper content of the formulations compared to the Marine Paint (40–50 % w/w Cu). Pre-loading the ligands with copper (before silica functionalisation) seems to result in a higher surface copper concentration then post-loading, but still not enough to achieve the desired bactericidal concentration on the surface despite leaching out similar amounts of copper as the marine paint. In fact, the pre-loaded Cu(II)-CnGmSiO_2/epx coated surface had the greatest number of viable adherent bacteria. Formulations including polyacylhydrazones were generally ineffective for the purposes of avoiding biofouling. On the other hand, that we identified beneficial effects with these systems, even without the presence of copper ions, implies that they retain potential to be used as sacrificial components of paints with the view to inhibiting the growth of organisms on those paint surfaces.

Acknowledgements: The research team is grateful for the support from the New Zealand Ministry of Business, Innovation and Science grant CONT-41762-SIP1-RSCHTRUSTVIC (Anti Foul Marine Paints) and HR for PhD funding secured therein. The authors thank Herbert Wong and Yinrong Lu (Callaghan Innovation) for providing nuclear magnetic resonance spectroscopy and mass spectrometry services. The assistance of Dr. Keith Clinch in organic synthetic methodology is gratefully acknowledged by HR.

References

[1] M. Vincent, R. E. Duval, P. Hartemann, M. Engels-Deutsch. *J. Appl. Microbiol.* **124**, 1032 (2018), https://doi.org/10.1111/jam.13681.
[2] D. Mitra, E.-T. Kang, K. G. Neoh. *ACS Appl. Mater. Interfaces* **12**, 21159 (2019), https://doi.org/10.1021/acsami.9b17815.
[3] I. Amara, W. Miled, R. B. Slama, N. Ladhari. *Environ. Toxicol. Pharmacol.* **57**, 115 (2018), https://doi.org/10.1016/j.etap.2017.12.001.
[4] K. Schiff, D. Diehl, A. Valkirs. *Mar. Pollut. Bull.* **48**, 371 (2004), https://doi.org/10.1016/j.marpolbul.2003.08.016.

[5] E. Ytreberg, M. Lagerström, S. Nöu, A.-K. E. Wiklund. *J. Environ. Manage.* **281**, 111846 (2021), https://doi.org/10.1016/j.jenvman.2020.111846.
[6] P. Buskens, M. Wouters, C. Rentrop, Z. Vroon. *J. Coat. Technol. Res.* **10**, 29 (2013), https://doi.org/10.1007/s11998-012-9456-0.
[7] J. Karlsson, E. Ytreberg, B. Eklund. *Environ. Pollut.* **158**, 681 (2010), https://doi.org/10.1016/j.envpol.2009.10.024.
[8] T. Schwartz, N. Schewe, M. Schwotzer, M. Heinle, A. Mahmood, P. Krolla, P. Thissen. *ACS Appl. Bio Mater.* **5**, 5190 (2022), https://doi.org/10.1021/acsabm.2c00616.
[9] C. E. Santo, N. Taudte, D. H. Nies, G. Grass. *Appl. Environ. Microbiol.* **74**, 977 (2008), https://doi.org/10.1128/aem.01938-07.
[10] E. Ladomersky, M. J. Petris. *Metallomics* **7**, 957 (2015), https://doi.org/10.1039/c4mt00327f.
[11] P. Pallavicini, G. Dacarro, Y. A. Diaz-Fernandez, A. Taglietti. *Coord. Chem. Rev.* **275**, 37 (2014), https://doi.org/10.1016/j.ccr.2014.04.013.
[12] A. M. Daines, H. Robinson, M. Glenny, D. B. G. Williams, S. F. Hinkley. *Prog. Org. Coat.* **121**, 38 (2018), https://doi.org/10.1016/j.porgcoat.2018.04.019.
[13] D. Zha, L. You. *ACS Appl. Mater. Interfaces* **8**, 2399 (2016), https://doi.org/10.1021/acsami.5b11552.
[14] C. Gros, F. Rabiet, F. Denat, S. Brandès, H. Chollet, R. Guilard. *J. Chem. Soc., Dalton Trans.* 1209–1214 (1996), https://doi.org/10.1039/DT9960001209.
[15] H.-T. Lu. *Colloid J.* **75**, 311 (2013), https://doi.org/10.1134/s1061933x13030125.
[16] H. F. Bereczki, L. Daróczi, I. Fábián, I. Lázár. *Microporous Mesoporous Mater.* **234**, 392 (2016), https://doi.org/10.1016/j.micromeso.2016.07.026.
[17] J. A. Barreto, M. Matterna, B. Graham, H. Stephan, L. Spiccia. *New J. Chem.* **35**, 2705 (2011), https://doi.org/10.1039/c1nj20558g.
[18] D. B. G. Williams, A. Cullen. *J. Org. Chem.* **74**, 9509 (2009), https://doi.org/10.1021/jo9020437.
[19] C. Jones. Bonding in transition metal complexes, in *d-and f-Block Chemistry*, pp. 97–129, Royal Society of Chemistry, New York (2001).
[20] M. C. Rodríguez-Argüelles, R. Cao, A. M. García-Deibe, C. Pelizzi, J. Sanmartín-Matalobos, F. Zani. *Polyhedron* **28**, 2187 (2009), https://doi.org/10.1016/j.poly.2008.12.038.
[21] M. T. S. Amorim, S. Chaves, R. Delgado, J. J. F. da Silva. *J. Chem. Soc., Dalton Trans.* 3065 (1991), https://doi.org/10.1039/dt9910003065.
[22] H. Ozay, Y. Baran, H. Miyamae. *J. Coord. Chem.* **64**, 1469 (2011), https://doi.org/10.1080/00958972.2011.574128.
[23] S. C. Lee, R. M. Izatt, X. X. Zhang, E. G. Nelson, J. D. Lamb, P. B. Savage, J. S. Bradshaw. *Inorg. Chim. Acta* **317**, 174 (2001), https://doi.org/10.1016/s0164-1212(00)00110-2.
[24] C. V. Esteves, P. Lamosa, R. Delgado, J. Costa, P. Désogère, Y. Rousselin, C. Goze, F. Denat. *Inorg. Chem.* **52**, 5138 (2013), https://doi.org/10.1021/ic400015v.
[25] S. Füzerová, J. Kotek, I. Císařová, P. Hermann, K. Binnemans, I. Lukeš. *Dalton Trans.* 2908 (2005), https://doi.org/10.1039/b507062g.
[26] L. M. Lima, D. Esteban-Gómez, R. Delgado, C. Platas-Iglesias, R. l. Tripier. *Inorg. Chem.* **51**, 6916 (2012), https://doi.org/10.1021/ic300784v.
[27] S. Lacerda, M. P. Campello, I. C. Santos, I. Santos, R. Delgado. *Polyhedron* **26**, 3763 (2007), https://doi.org/10.1016/j.poly.2007.04.037.
[28] L. Wang, Y. Ye, V. Lykourinou, J. Yang, A. Angerhofer, Y. Zhao, L. J. Ming. *Eur. J. Inorg. Chem.* **2017**, 4899 (2017), https://doi.org/10.1002/ejic.201700811.
[29] M. Michailidis, I. Sorzabal-Bellido, E. A. Adamidou, Y. A. Diaz-Fernandez, J. Aveyard, R. Wengier, D. Grigoriev, R. Raval, Y. Benayahu, R. A. D'Sa. *ACS Appl. Mater. Interfaces* **9**, 38364 (2017), https://doi.org/10.1021/acsami.7b14642.
[30] J. Bentley, G. P. A. Turner. in *Introduction to Paint Chemistry and Principles of Paint Technology*, CRC Press, Boca Raton (1997).
[31] F. Ortega, E. Velez, R. Somanathan. *J. Chem. Educ.* **73**, A26 (1996), https://doi.org/10.1021/ed073pa26.
[32] R. J. Corriu, F. Embert, Y. Guari, C. Reyé, R. Guilard. *Chem. – Eur. J.* **8**, 5732 (2002), https://doi.org/10.1002/1521-3765(20021216)8:24<5732::aid-chem5732>3.0.co;2-h.
[33] R. J. Corriu, A. Mehdi, C. Reyé, C. Thieuleux. *Chem. Mater.* **16**, 159 (2004), https://doi.org/10.1021/cm034903d.
[34] S. Goubert-Renaudin, M. Etienne, S. Brandès, M. Meyer, F. Denat, B. Lebeau, A. Walcarius. *Langmuir* **25**, 9804 (2009), https://doi.org/10.1021/la900892q.
[35] P. Pallavicini, G. Dacarro, L. Cucca, F. Denat, P. Grisoli, M. Patrini, N. Sok, A. Taglietti. *New J. Chem.* **35**, 1198 (2011), https://doi.org/10.1039/c0nj00829j.
[36] S. Warnes, V. Caves, C. Keevil. *Environ. Microbiol.* **14**, 1730 (2012), https://doi.org/10.1111/j.1462-2920.2011.02677.x.
[37] G. Grass, C. Rensing, M. Solioz. *Appl. Environ. Microbiol.* **77**, 1541 (2011), https://doi.org/10.1128/aem.02766-10.
[38] J. Stevenson, A. Barwinska-Sendra, E. Tarrant, K. Waldron. *Microbial Pathog. Strat. Combat. Them: Sci. Technol. Educ.* **2**, 468 (2013).
[39] M. Hans, S. Mathews, F. Mücklich, M. Solioz. *Biointerphases* **11**, 018902 (2016), https://doi.org/10.1116/1.4935853.
[40] L. Macomber, J. A. Imlay. *Proc. Natl. Acad. Sci. U. S. A.* **106**, 8344 (2009), https://doi.org/10.1073/pnas.0812808106.
[41] W. Teughels, N. Van Assche, I. Sliepen, M. Quirynen. *Clin. Oral Implants Res.* **17**, 68 (2006), https://doi.org/10.1111/j.1600-0501.2006.01353.x.
[42] A. Kozlovsky, Z. Artzi, O. Moses, N. Kamin-Belsky, R. B. N. Greenstein. *J. Periodontol.* **77**, 1194 (2006), https://doi.org/10.1902/jop.2006.050401.

Supplementary Material: This article contains supplementary material (https://doi.org/10.1515/pac-2024-0203).